

Wearable Sensors Based on Solid-Phase Molecular Self-Assembly: Moisture-Strain Dual Responsiveness Facilitated Extremely High and Damage-Resistant Sensitivity

Tongyue Wu, Shuitao Gao, Wenkai Wang, Jianbin Huang, and Yun Yan*

Cite This: *ACS Appl. Mater. Interfaces* 2021, 13, 41997–42004

Read Online

ACCESS |

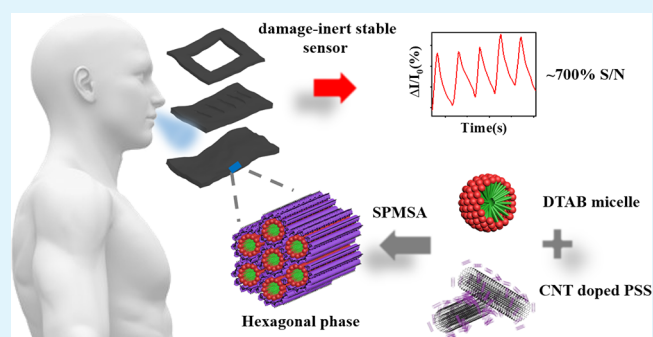
Metrics & More

Article Recommendations

Supporting Information

ABSTRACT: Wearable sensing technologies have gained increasing interest in biomedical fields because they are convenient and could efficiently monitor health conditions by detecting various physiological signals in real time. However, common film sensors often neglect body moisture and enhance the sensitivity by enhancing the conductive dopants and self-healing ability. We report in this work a supramolecular film sensor based on solid-phase molecular self-assembly (SPMSA), which smartly utilizes the body moisture to enhance the sensitivity for human-machine interaction. The carbon nanotube (CNT)-doped SPMSA film is able to capture environmental moisture quickly. Upon contact to human skin, the moisture not only promotes the junction between CNTs but also contributes to the conductivity. As a result, the sensitivity can be enhanced 4 times. In this way, we are able to obtain the highest sensitivity of 700% with the lowest CNT doping rate of 0.5%. Furthermore, the current sensor displays damage-inert sensing performance. In the presence of a hole of up to 50% of the film area, the sensitivity remains unaffected due to the decreases in the absolute conductivity of the film sensor before and after a trigger to the same extent. In this way, we have developed a new principle in the design of a film sensor for human-machine interaction, which releases the sensor from focus on promoting conductivity and self-healing materials.

KEYWORDS: solid-phase molecular self-assembly (SPMSA), moisture–strain dual response, high sensitivity, damage resistant, wearable sensor



1. INTRODUCTION

Smart human-machine interaction is attracting tremendous attention in diversified fields of modern society such as wearable electronics, health care, and soft robotics.¹ Flexible sensors capable of transducing physical strains into electrical signals are of significant importance for effective human-machine interactions. An ideal sensor for these purposes should display both excellent sensitivity and flexibility. To meet these requirements, people have endeavored to design various conductive soft materials.^{2–4} Soft materials used in wearable sensors are often flexible polymer films resulting from solvent evaporation⁵ or hydrogels.^{6–8} Except for flexible films made with elegantly designed conductive polymers,^{9,10} few soft materials are intrinsically conductive. For this reason, carbon nanotubes,^{11–13} graphene,^{14–16} silver nanowires,^{17–19} inorganic salts,^{20–22} and ionic liquids^{23,24} were often doped to achieve desired conductivity. Inkjet printing,²⁵ laser manufacturing,²⁶ and 3D printing of these materials on a soft substrate²⁵ were also employed to create patterned sensors. Because of the high reliance on mechanical engineering background that is lacked by most chemists, the chemical

doping method is extensively employed in the field of chemistry to prepare various wearable sensors.

At present, carbon nanotubes (CNTs) are extensively used as conductive dopants owing to their high intrinsic carrier mobility, excellent conductivity, and mechanical flexibility.²⁷ It is generally believed that high conductivity is advantageous for better sensitivity.^{5,27} People usually try to dope a significant amount of CNTs, often higher than 5%, to acquire better signal sensing ability. However, the sensing signal (SS) is expressed by the ratio between the variation of the current (or conductivity) triggered by a strain and the absolute conductivity.^{5,28} This inspires the idea that a key for better sensing is to enhance the extent of conductivity variation rather than to improve the absolute conductivity of a soft material.

Received: June 9, 2021

Accepted: August 18, 2021

Published: August 25, 2021



Scheme 1. (a) Fabrication Process of the DTAB-PSS-CNT-Urea Composite Film; (b) Photo of a Newly Obtained DTAB-PSS-CNT-Urea Conductive Film

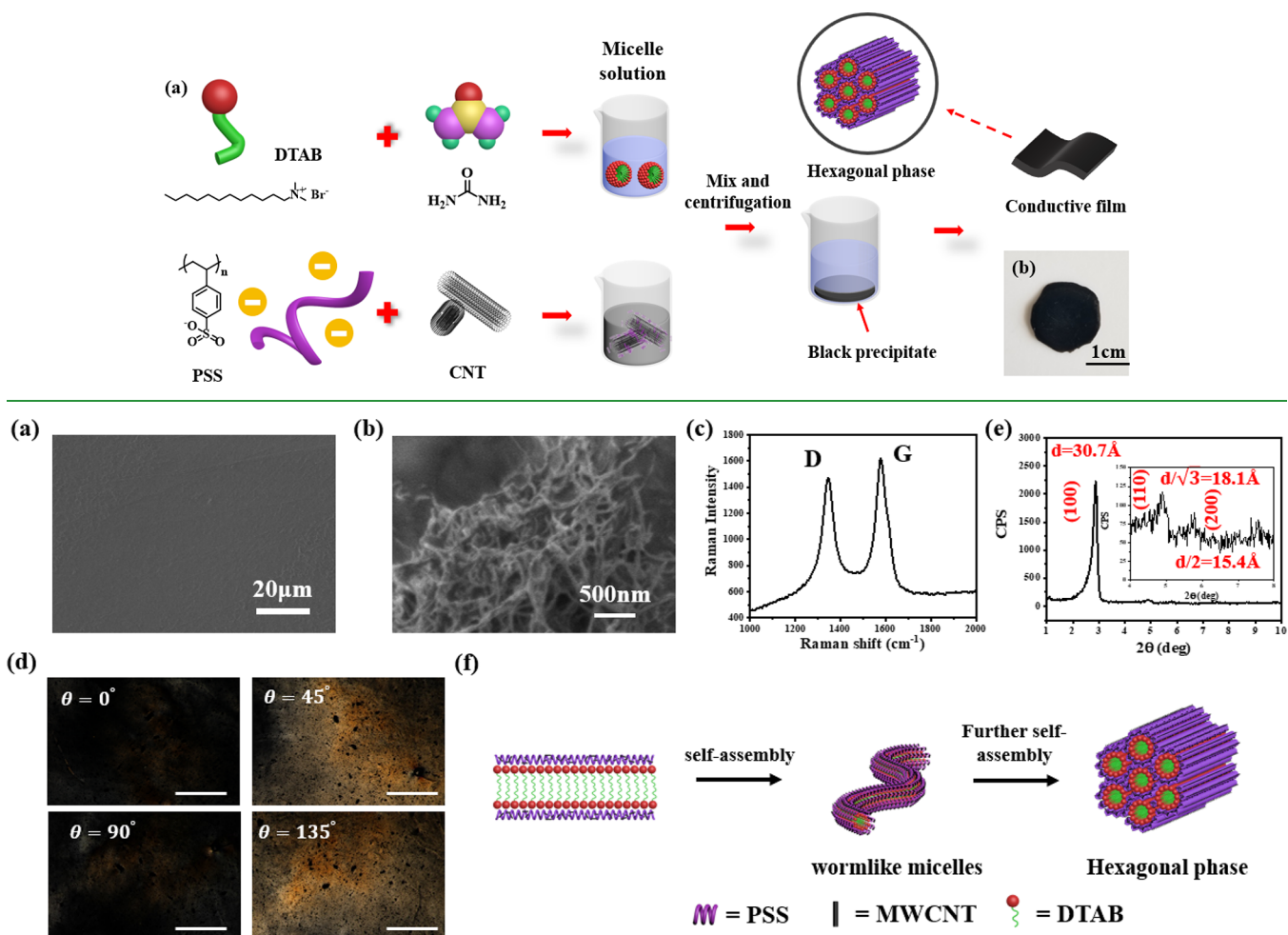


Figure 1. SEM image of the DTAB-PSS-CNT-urea conductive film from (a) the surface and (b) cross-section. (c) Micro-Raman spectrum of the DTAB-PSS-CNT-urea film (laser wavelength: 532 nm). (d) POM images of the DTAB-PSS-CNT-urea film aligned at various angles relative to two surrounding vertically arranged polarizers (scale bar: 100 μm). (e) XRD pattern of the DTAB-PSS-CNT-urea film (storage humidity: 100%). (f) Systematical illustration of the DTAB-PSS-CNT-urea film formation process.

Human body contains a large quantity of water. Many body movements not only involve a mere change in physical strains but are also often accompanied by variation in water vapor. For instance, a deep breath is accompanied by the enhanced vapor content in the expiration; clenched fists usually occur together with a sweaty hand. Clearly, if the conductivity of a sensor could reflect both the variation in physical strains and the accompanied moisture variation, a significantly enhanced sensing signal would be expected. However, most polymer films are usually moisture resistant so those cannot respond to environmental moisture, whereas the hydrogel films are not sensitive to moisture due to the presence of tremendous water in the film. So far, it still remains challenging to design a wearable sensor that could real-time capture both the moisture and strain variation of human body synchronously.

Herein, we report the creation of CNT-doped supramolecular film sensors using the strategy of solid-phase molecular self-assembly (SPMSA) recently developed in our lab.^{29,30} In this strategy, a precipitate is created from the aqueous solution of oppositely charged surfactant and polyelectrolyte. Under mechanical pressure, the precipitate will transform into a continuous supramolecular film owing to

the merging of the surfactant domains bridged by the polyelectrolyte chains. Because the ionic groups of the surfactant and polyelectrolyte are prone to adsorb moisture from surroundings quickly, the flexibility of the film increases drastically. Consequently, the junction between the CNTs becomes more sufficient, which leads to a drastic increase in conductivity. As such, both the strain and moisture-triggered conductivity change would contribute to the sensing signal. It is striking that the signals generated by a naked finger pressing is nearly 25 times higher than that from a gloved one. Since body moisture variation, such as sweat, is often accompanied with the physical and physiological status of people, it is very promising for real-time monitoring of the physical status of a patient, athlete, and the physiological status of investigated people. With the assistance of moisture responsive conductivity, the maximum sensing signal (SS) for a film with 0.5% CNTs can be enhanced to 700%, which is in clear contrast to the literature results for the 0–400% SS achieved with 30–100% CNTs.^{31–37} Finally, we found that the sensitivity of the current film sensor is even not affected by the presence of a hole that occupies 50% the film surface, probably due to the same amplitude of variation of the current

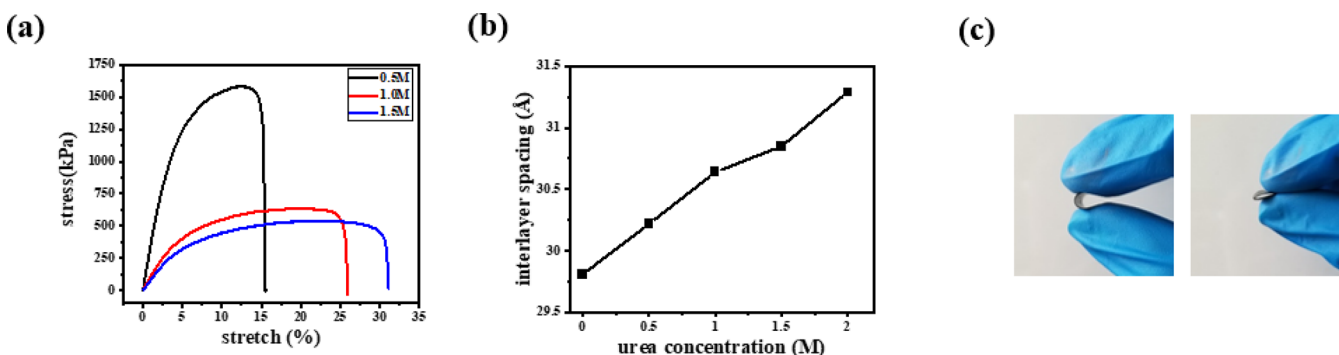


Figure 2. (a) Stress–strain curve of the conductive film with different contents of urea. (b) Interlayer spacing varies with different concentrations urea. (c) Actual bending and folding performance of the film.

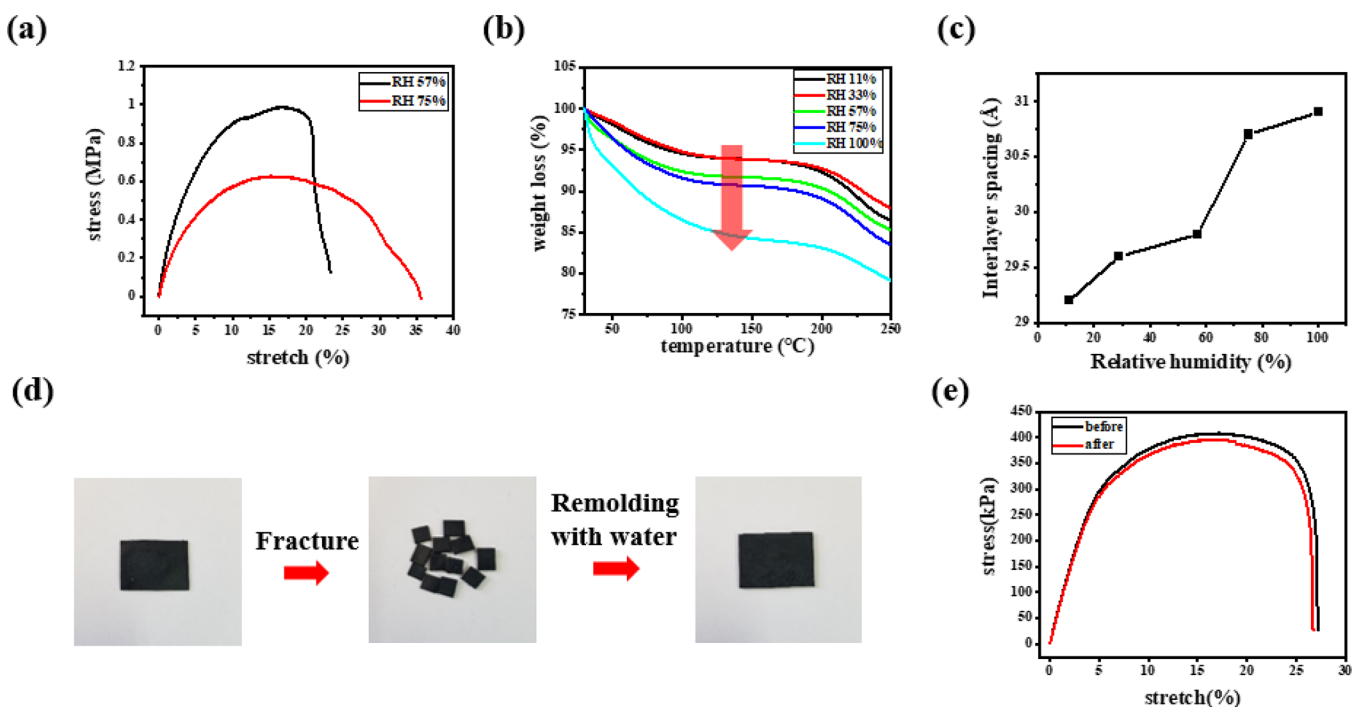


Figure 3. (a) Mechanical strength characteristics under different humidities. (b) TGA tests and (c) interlayer spacing results for different storage conditions. (d) Plasticity of films. (e) Comparison of tensile properties before and after film remodeling. After remodeling, the film still possesses certain deformability and tensile strength.

change and absolute current triggered by the damage. In this sense, we have constructed a damage-inert super sensitive skin-like strain sensor without endeavoring to the self-healing ability. We expect that the current strategy of solid-phase molecular self-assembly would be very promising in human-machine interactions.

2. RESULTS AND DISCUSSIONS

2.1. Preparation of a Multifunctional Film.

The fabrication process of this DTAB-PSS-CNT-urea (DTAB, *N,N,N*-trimethyl-1-dodecanaminium bromide, PSS, and poly(sodium styrenesulfonate)) film is demonstrated in Scheme 1a. CNTs were first dispersed in the aqueous solution of PSS under sonication. In this way, PSS would wrap on the surface of CNTs like a carpet.³⁸ This black dispersion was then mixed with the aqueous solution of DTAB (Figure S1) containing urea under stirring. Under mechanical pressure, the fresh precipitates immediately transform into a black self-supporting film (Scheme 1b). Urea is critical for the film formation since it

enhances the water-preserving ability so that the molecules in the pressed precipitates are able to rearrange sufficiently to form a bulk film. Without addition of urea, pressing the precipitates only results in a coarse cake. In the presence of sufficient urea, the content of CNT can be varied in the range of 0–2% (Figure S2). Further enhancing the content of CNTs leads to failure of film formation. It should be clarified that if no CNT is involved, pressing the precipitate formed with DTAB-PSS is enough to generate a film, which is the general property of most pairs of oppositely charged surfactants/polyelectrolytes as reported in our previous work.²⁹ In the current study, the fresh DTAB-PSS film is white, which is not conductive due to the lack of conductive dopants (Figure S3).

2.2. Characterization of the Prepared Film.

The surface of the film with 0.5% CNT under SEM is rather flat (Figure 1a), but the image for the cross-section clearly revealed the presence of networks formed with CNTs (Figure 1b). The Raman spectrum gives typical D and G bands for multiwalled CNTs (Figure 1c). X-ray photoelectron spectroscopy (XPS,

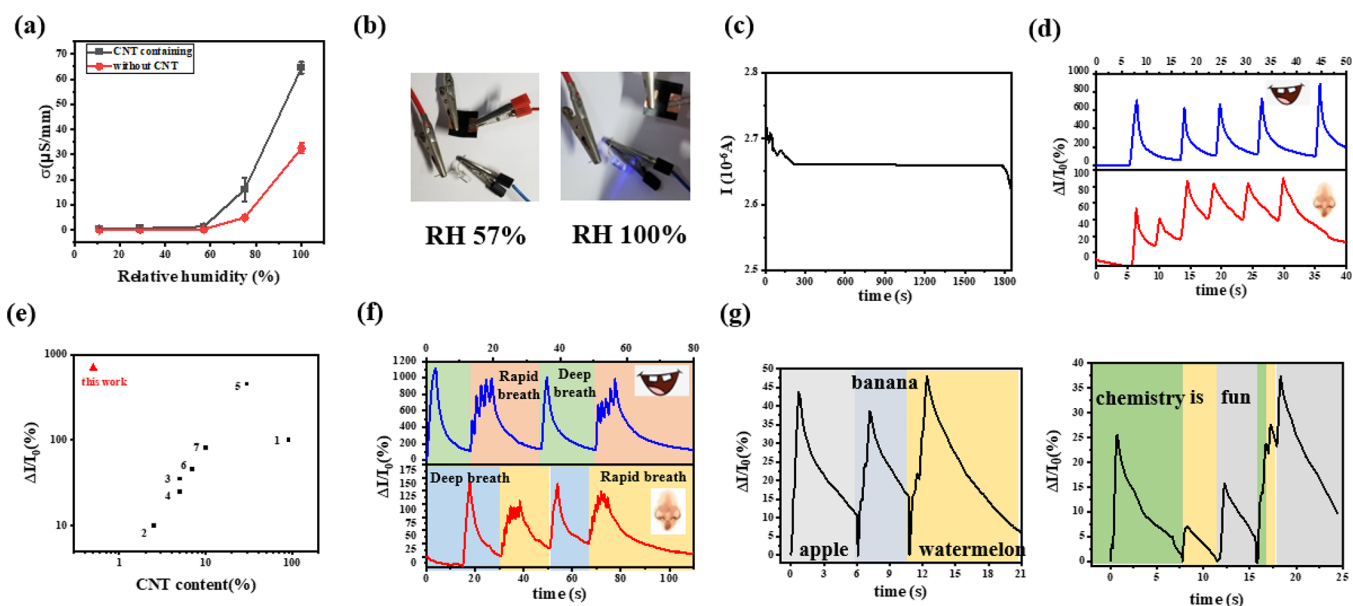


Figure 4. (a) Relationship between film conductivity (with and without CNTs) and storage humidity. (b) Film can light up an LED of 0.05 W when humidity is above 75%. (c) Conductivity of the film remains stable under 30 min of measurement (ambient humidity: 55%). (d) Continuous breathing response curves from mouth (upper panel) and nose (lower panel). (e) Comparison of the CNT doping amount and sensitivity of DTAB-PSS-CNT in this work with the results in other literature reports (X axis corresponds to CNT content and Y axis corresponds to respond sensitivity). (1: [36], 2: [31], 3: [32], 4: [33], 5: [35], 6: [37], and 7: [34]). (f) Response curves from different mouth (upper panel) and nose (lower panel) breathing rates. (g) Film is able to distinguish different words and sentences.

Figure S4), ^1H NMR measurements (Figure S5), thermogravimetric analysis (TGA, Figure S6), and elemental analysis (Table S1) suggest that the molar ratio between DTAB, PSS, and urea in the film is 1.15:1.00:0.24. For a film with thickness smaller than 200 μm , strong extinction was observed under a polarized optical microscope (POM). As the samples in between two vertically oriented polarizers were aligned at angles of 0 and 90° relative to the polarizers, the brightest birefringence was observed when angles were 45 and 135° (Figure 1d), indicating the presence of a large area of ordered liquid crystalline mesophases in the film. In line with this, a sharp and intensive diffraction peak was observed in the XRD measurement, which is followed by two extra weak diffractions. The three diffractions acquired a spacing ratio of 1: $\sqrt{3}$: $\sqrt{4}$, corresponding to (100), (110), and (200) diffractions of the Miller Indices of a 2D hexagonal mesostructure (Figure 1e). The spacing obtained from the (100) diffraction is about 3.0 nm, which is about 2 times of the stretching length of DTAB. This means that the DTAB molecules in the film have formed wormlike micelles,^{22,23} which further packed into hexagonal phases (Figure 1f). The PSS-wrapped CNTs were then lying on the surface of the DTAB bilayers owing to the electrostatic interactions, as demonstrated in Figure 1f.

2.3. Influence of Urea on the Mechanical Properties of the Film. To test the ability of the film being used as conductive strain sensors, the mechanical property of the film was examined. We found that for a given doping amount of CNTs, the mechanical property of the film is closely related with the content of urea and environmental humidity. Without addition of urea, pressing the precipitates simply leads to a cake with a coarse surface. An intact film can be obtained as a certain amount of urea is added into the DTAB solution. Figure 2a shows that as the content of urea increases from 0.5 to 1.5 M, the flexibility of the film increases from 15 to 30%, whereas the mechanical strength decreases from 1.5 to 0.5

MPa. XRD measurements (Figure 2b) reveal that the increased fraction of urea in the film has increased the interlayer spacings, suggesting that the urea molecules have inserted in the hydrophilic layers in the film (Figures S7 and S8). It is noticed that the film with 15% stretchability, which has the highest mechanical strength, is flexible enough. This film can be arbitrarily bent and folded without fractures (Figure 2c), which makes it qualified for the application as flexible sensors. Therefore, the film with 0.5 M urea was used in the following studies.

2.4. Influence of Environmental Moisture on the Mechanical Properties of the Film. Figure 3a shows that as the environmental humidity increases, the mechanical strength of the film decreases. Thermogravimetric analysis (TGA) measurements revealed that the water content in the film increases with increasing environmental humidity (Figure 3b). The XRD patterns in Figure 3c suggest that the interlayer spacings increase with water content, indicating binding of the water molecules with the ionic groups.²² These water molecules also endow the DTAB-PSS-CNT-urea film with good plasticity. As wetted by water, it can be regenerated repeatedly under proper mechanical pressure regardless of what damage it has suffered (Figure 3d). The mechanical strength of the regenerated film remains the same as that of the original one (Figure 3e).

2.5. Moisture-Responsive Conductivity of the Film. The conductivity of the film displays distinct humidity responsiveness. The film with 0.5% CNT displays only very low conductivity as the RH (relative humidity) is below 57% (Figure 4a), which cannot light up the 0.05 W LED. However, at humidity above 57%, a drastic conductivity increase occurs. Figure 4b shows that when a film at the humidity of 57% failed to light up a LED, increasing the humidity to 100% successfully did so. Control experiments in Figure 4a suggested that the conductance for the film without CNTs under the same

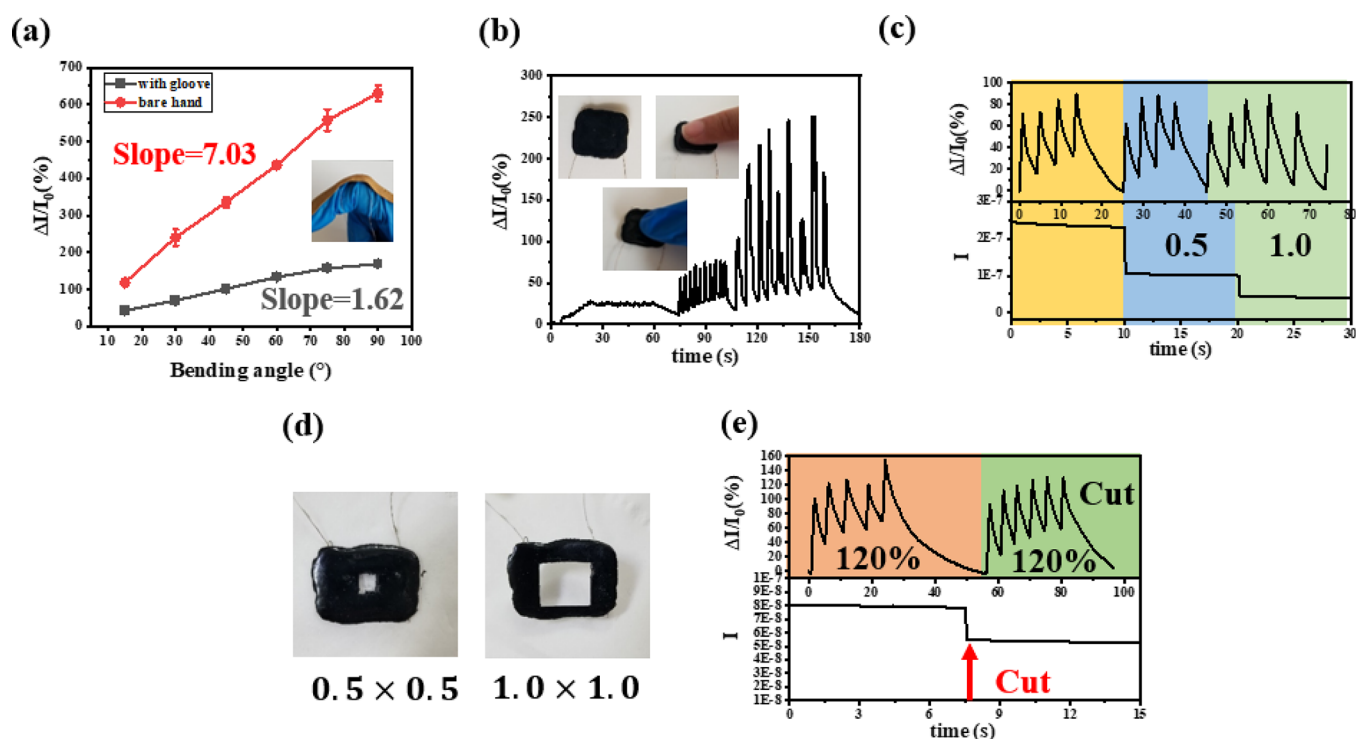


Figure 5. (a) Response curve of different finger joint bending angles with a glove and directly using a bare hand. Inset: bending detecting method. (b) Response to finger pressing with gloves, dry, and wet hand. Inset: different pressing states. (c) Response of the film to oral respiration under different degrees of damage. (d) Photo of the hole of different sizes. (e) Effect of a scratch (scratch length: 1.0 cm) on the signal response and absolute current.

situation is about half of that with CNTs, indicating that both the better junction between the CNTs in the film and water have contributed to the conductivity. It is noticed that the conductive signal remains stable within 30 min (Figure 4c), so water evaporation during the measuring process can be neglected.

Although the sensing signal decreases with increasing humidity (Figure S9), it is striking to find that the conductivity of the film prepared at 57% RH displays instant moisture responsiveness. As the film is subjected to breath from nose and mouth, respectively, the conductive signals are drastically different (Figure 4d). Since breath from mouth has more moisture, the sensing signal can be as high as 700%, which is nearly 10 times of the 80% current variance generated by the nose breath. It is noticed that compared with literature results, the current work gives the highest sensitivity to respiration with the lowest CNT doping rate (Figure 4e). The extremely high current variance of 700% in this work is achieved only with 0.5% CNTs, which is in clear contrast with the best literature reports of the 100–400% current variance obtained with the 60 and 200 times higher CNT doping rates of 30 and 100%. This result indicates that increasing the conductivity of the soft materials only offers limited help in promoting the sensing ability; the assistance of moisture responsive sensing is very significant in providing high sensing ability.

This quick responsiveness toward moisture enables the film to be used in real time to monitor any small moisture variation. Figure 4f shows that for a rapid breath, the sensing signal displays multiple peaks, whereas that for a deep breath is rather smooth. With this extremely high moisture sensitivity, the film is even able to distinguish speaking of words with different syllables. For example, when reading a three-syllable word,

“banana”, three consecutive current peaks can be detected, while for words with more syllables, like “watermelon”, a more complex waveform result is shown (Figure 4g). In addition to identifying simple words, DTAB-PSS-CNT-urea films can also achieve the goal of effective recognition of sentences. As shown in Figure 4g, each word can be effectively detected and distinguished whether the sentence is read separately or continuously. This kind of special recognition ability of words and sentences is very helpful for the communication of patients suffering from hearing ability.

2.6. Moisture-Strain Dual Responsiveness of the Film.

To test whether the film can be used as moisture-strain dual responsive wearable sensors for human-machine interactions, the conductivity responsiveness toward physical strain is measured for the bending of a human finger. To avoid the influence from the skin moisture, the finger was protected by a glove. Figure 5a shows that as the film is attached to the gloved finger, the sensing signal increases proportionally with the bending extent. As the glove is taken off to allow direct adhering of the film to the finger, the slope of the sensing signal–bending curve increases more than 4 times, indicating that the sensitivity have been promoted 4 times. Clearly, the skin moisture has facilitated to enhance the sensing signal. It is therefore validated that the film displays moisture-strain dual sensing ability.

To demonstrate the advantages of the dual responsiveness in practical human-machine interaction, the conductivity changes of the film triggered by a gloved finger, a naked finger, and a sweaty finger is compared. Figure 5b shows that when the sensor was introduced to a circuit, pressing the film with a gloved finger can only generate a weak conductive response of about 10%. However, as the glove is taken off, the sensing

signal amounted to 75%. Strikingly, as the finger was sweaty, the same pressing action would generate a drastically enhanced sensing signal of 250%. This sweat triggered a 25 times larger conductive response, unambiguously manifesting that the current film is an excellent flexible sensor in detecting body movements that involves moisture change.

Finally, but most strikingly, the film displays damage-inert stable sensing behavior (Figure 5c,d). As a hole was made in the film, the sensing signal of breathing remains unchanged compared with the original one. The sensing performance is so reliable that as the area of the hole is about 50% of the film, the sensing signal remains the same. Records for the absolute current variation indicate that the damage would cause a decrease in the absolute current but not the relative variance of the conductivity. This means that the damage has changed the original and triggered conductivity in the same amplitude. To the best of our knowledge, it is the first damage-inert sensing behavior ever reported. We envision that the current humidity-strain dual sensing film protrudes promising potential in the field of human-machine interaction.

3. CONCLUSIONS

In conclusion, we have developed a multifunctional smart sensing system, DTAB-PSS-CNT-urea, using the strategy of solid-phase molecular self-assembly (SPMSA) for real-time health monitoring. The ability to retain water renders the film with dual responsive conductivity toward humidity and mechanical strain. The humidity responsiveness on the one hand is beneficial for a better CNT junction and on the other hand provides extra conductivity for the film. Since the surface of a human body always has a moist environment, the extra humidity responsiveness endows the film with 4 times enhanced excellent sensing ability. With this extra humidity facilitated conductivity enhancement, the current film achieves the highest sensing performance with the lowest doping of 0.5% CNTs. Furthermore, we found that for a real-time human-machine interaction, the relative conductivity variance, which is the output sensing signal, remains constant in the presence of film damages. In this sense, the current work discloses a new sensing mode that positively utilizes the physical moisture variation, as well as the damage-inert sensing performance. We envision that the current design would open a new vista in the design of smart sensors for human-machine interactions.

4. MATERIALS AND METHODS

4.1. Materials. *N,N,N*-Trimethyl-1-dodecanaminium bromide (DTAB) and sodium polystyrene sulfonate (PSS, M_n : 70,000) were purchased from the Sigma-Aldrich Corporation. The multiwalled carbon nanotube (MWCNT) is provided by other laboratories. Silver conductive paint is from SPI, USA. All other reagents were of AR grade. Deionized water (18.2 M Ω cm) was from the ELGA PURELAB classic system.

4.2. Film Fabrication. PSS (0.1 mol/dm³, about 2 wt %) was completely dissolved at 50 °C, then 0.2 wt % MWCNT was added, and ultrasonic treatment was performed at room temperature for 60 min till all the MWCNTs dispersed uniformly. Urea was added into the 0.1 mol/dm³ DTAB solution until it reached a concentration of 0.5 mol/dm³. After complete dissolution, the solutions were stored at room temperature waiting to be used.

The solution containing PSS and MWCNTs were poured into the DTAB solution to reach electrostatic balance. Black precipitates formed immediately. The precipitates were collected after centrifuging for 5 min at 8000 rpm. Under a mild mechanical pressure, the black

precipitates were transformed into a smooth film that was cut into desired shapes with scissors or blade for testing.

4.3. Sensing Device Fabrication. The cut film was connected into a circuit to fabricate a sensing device by gluing silver wire with silver glue onto it with an electrochemical workstation. All newly prepared sensors were stored at a 57% RH environment before use.

4.4. Characterization and Measurements. Scanning electron microscopy (SEM, Hitachi S-4800) was employed to observe the morphology of the conductive film at an acceleration voltage of 1 kV. Energy-dispersive spectroscopy (EDS) measurement was conducted using the same instrument at an acceleration voltage of 7 kV. X-ray diffraction (XRD) measurements were performed using a Rigaku D/max-2400 diffractometer (Tokyo, Japan) with Cu K α radiation. Polarized microscopy (POM) was performed with an LV100N polarizing microscope (Nikon Co., Irving, CA) under ambient environmental conditions. A WDW3020 electronic universal testing machine is used for the measurement of the mechanical properties of the films. Stress-strain data were collected with a strain rate of 10 mm/min. All mechanical tests were conducted with dumbbell-shaped samples. Thermogravimetric analysis (TGA) experiments were carried out under nitrogen flow on a TA Instrument Q600 SDT at a heating rate of 10 °C/min. A micro-Raman imaging spectrometer (DXRxi) was used for the Raman spectrum of MWCNTs via a 532 nm laser. The I-t scanning mode of the electrochemical workstation was used to measure the multiple responses of the film with a voltage setting at 0.5 V. An MY65 multimeter (MASTECH) was used for resistance measurement under different conditions. The saturated inorganic salt solution was used to control the humidity, and an Xs105 electronic balance (Mettler Toledo) was used to measure the exact weight at the specified time to record the water absorption and loss rate of the film. An Hy3005et DC power supply (HYELEC) was used for film conductivity detection. Nuclear magnetic resonance (NMR) analysis was conducted using a Bruker400 MHz NMR. The infrared spectrum can be obtained using a Spectrum Spotlight 200 FT-IR microscopy system. XPS was performed using an AXIS Supra X-ray photoelectron spectrometer, N and C elements are the main focus elements.

All experiments without special notation were carried out at a 57% RH environment.

■ ASSOCIATED CONTENT

Supporting Information

The Supporting Information is available free of charge at <https://pubs.acs.org/doi/10.1021/acsami.1c10717>.

DLS results for DTAB solution; variation of the content of CNT on the conductivity of the film; XPS, HNMR, elemental analysis, TGA, Infrared spectra, and EDS results for the PSS-DTAB-urea film; factors affecting the response amplitude of DTAB-PSS-MWCNT-urea films; the relationship between CNT content and signal response amplitude; of continuous speech recognition; and repeatability of a response (PDF)

■ AUTHOR INFORMATION

Corresponding Author

Yun Yan – College of Chemistry and Molecular Engineering, Peking University, Beijing 100871, China; orcid.org/0000-0001-8759-3918; Email: yunyan@pku.edu.cn

Authors

Tongyue Wu – College of Chemistry and Molecular Engineering, Peking University, Beijing 100871, China
Shuitao Gao – College of Chemistry and Molecular Engineering, Peking University, Beijing 100871, China
Wenkai Wang – College of Chemistry and Molecular Engineering, Peking University, Beijing 100871, China

Jianbin Huang – College of Chemistry and Molecular Engineering, Peking University, Beijing 100871, China

Complete contact information is available at:
<https://pubs.acs.org/10.1021/acsami.1c10717>

Author Contributions

The manuscript was written through contributions of all authors. All authors have given approval to the final version of the manuscript.

Notes

The authors declare no competing financial interest.

ACKNOWLEDGMENTS

The authors are grateful to the National Natural Science Foundation of China (grant no. 91856120, 21573011, and 21633002) and the Beijing National Laboratory for Molecular Sciences (BNLMS) for financial support.

REFERENCES

- (1) Hsieh, H. H.; Hsu, F. C.; Chen, Y. F. Energetically Autonomous, Wearable, and Multifunctional Sensor. *ACS Sens.* **2018**, *3*, 113–120.
- (2) He, H.; Li, Y.; Liu, H.; Kim, Y.; Yan, A.; Xu, L. Elastic, Conductive, and Mechanically Strong Hydrogels from Dual-Cross-Linked Aramid Nanofiber Composites. *ACS Appl. Mater. Interfaces* **2021**, *13*, 7539–7545.
- (3) Yiming, B.; Han, Y.; Han, Z.; Zhang, X.; Li, Y.; Lian, W.; Zhang, M.; Yin, J.; Sun, T.; Wu, Z.; Li, T.; Fu, J.; Jia, Z.; Qu, S. A Mechanically Robust and Versatile Liquid-Free Ionic Conductive Elastomer. *Adv. Mater.* **2021**, 2006111.
- (4) Wang, X.; Chen, G.; Cai, L.; Li, R. A.; He, M. Weavable Transparent Conductive Fibers with Harsh Environment Tolerance. *ACS Appl. Mater. Interfaces* **2021**, *13*, 8952–8959.
- (5) Tsai, Y. J.; Wang, C. M.; Chang, T. S.; Sutradhar, S.; Chang, C. W.; Chen, C. Y.; Hsieh, C. H.; Liao, W. S. Multilayered Ag NP-PEDOT-Paper Composite Device for Human-Machine Interfacing. *ACS Appl. Mater. Interfaces* **2019**, *11*, 10380–10388.
- (6) Liu, X.; Zhang, Q.; Gao, G. Solvent-Resistant and Nonswellable Hydrogel Conductor toward Mechanical Perception in Diverse Liquid Media. *ACS Nano* **2020**, *14*, 13709–13717.
- (7) Guan, L.; Yan, S.; Liu, X.; Li, X.; Gao, G. Wearable strain sensors based on casein-driven tough, adhesive and anti-freezing hydrogels for monitoring human-motion. *J. Mater. Chem. B* **2019**, *7*, 5230–5236.
- (8) Jiao, Q.; Cao, L.; Zhao, Z.; Zhang, H.; Li, J.; Wei, Y. Zwitterionic Hydrogel with High Transparency, Ultradstretchability, and Remarkable Freezing Resistance for Wearable Strain Sensors. *Biomacromolecules* **2021**, *22*, 1220–1230.
- (9) Peng, Y.; Yan, B.; Li, Y.; Lan, J.; Shi, L.; Ran, R. Antifreeze and moisturizing high conductivity PEDOT/PVA hydrogels for wearable motion sensor. *J. Mater. Sci.* **2019**, *55*, 1280–1291.
- (10) Ren, K.; Cheng, Y.; Huang, C.; Chen, R.; Wang, Z.; Wei, J. Self-healing conductive hydrogels based on alginate, gelatin and polypyrrole serve as a repairable circuit and a mechanical sensor. *J. Mater. Chem. B* **2019**, *7*, 5704–5712.
- (11) Liu, Z.; Qi, D.; Leow, W. R.; Yu, J.; Xiloyannis, M.; Cappello, L.; Liu, Y.; Zhu, B.; Jiang, Y.; Chen, G.; Masia, L.; Liedberg, B.; Chen, X. 3D-Structured Stretchable Strain Sensors for Out-of-Plane Force Detection. *Adv. Mater.* **2018**, *30*, No. e1707285.
- (12) Li, Q.; Li, J.; Tran, D.; Luo, C.; Gao, Y.; Yu, C.; Xuan, F. Engineering of carbon nanotube/polydimethylsiloxane nanocomposites with enhanced sensitivity for wearable motion sensors. *J. Mater. Chem. C* **2017**, *5*, 11092–11099.
- (13) Meng, L.; Xu, Q.; Dan, L.; Wang, X. Single-Walled Carbon Nanotube Based Triboelectric Flexible Touch Sensors. *J. Electron. Mater.* **2019**, *48*, 7411–7416.
- (14) Zhang, H.; Ren, P.; Yang, F.; Chen, J.; Wang, C.; Zhou, Y.; Fu, J. Biomimetic epidermal sensors assembled from polydopamine-modified reduced graphene oxide/polyvinyl alcohol hydrogels for the real-time monitoring of human motions. *J. Mater. Chem. B* **2020**, *8*, 10549–10558.
- (15) Kamat, A. M.; Pei, Y.; Jayawardhana, B.; Kottapalli, A. G. P. Biomimetic Soft Polymer Microstructures and Piezoresistive Graphene MEMS Sensors Using Sacrificial Metal 3D Printing. *ACS Appl. Mater. Interfaces* **2021**, *13*, 1094–1104.
- (16) Li, Q.; Bai, R.; Gao, Y.; Wu, R.; Ju, K.; Tan, J.; Xuan, F. Laser Direct Writing of Flexible Sensor Arrays Based on Carbonized Carboxymethylcellulose and Its Composites for Simultaneous Mechanical and Thermal Stimuli Detection. *ACS Appl. Mater. Interfaces* **2021**, *13*, 10171–10180.
- (17) Herbert, R.; Lim, H. R.; Yeo, W. H. Printed, Soft, Nanostructured Strain Sensors for Monitoring of Structural Health and Human Physiology. *ACS Appl. Mater. Interfaces* **2020**, *12*, 25020–25030.
- (18) Kim, T.; Park, C.; Samuel, E. P.; An, S.; Aldalbah, A.; Alotaibi, F.; Yarin, A. L.; Yoon, S. S. Supersonically Sprayed Washable, Wearable, Stretchable, Hydrophobic, and Antibacterial rGO/AgNW Fabric for Multifunctional Sensors and Supercapacitors. *ACS Appl. Mater. Interfaces* **2021**, *13*, 10013–10025.
- (19) Jo, H. S.; An, S.; Park, C. W.; Woo, D. Y.; Yarin, A. L.; Yoon, S. S. Wearable, Stretchable, Transparent All-in-One Soft Sensor Formed from Supersonically Sprayed Silver Nanowires. *ACS Appl. Mater. Interfaces* **2019**, *11*, 40232–40242.
- (20) Yu, J.; Dang, C.; Liu, H.; Wang, M.; Feng, X.; Zhang, C.; Kang, J.; Qi, H. Highly Strong and Transparent Ionic Conductive Hydrogel as Multifunctional Sensors. *Macromol. Mater. Eng.* **2020**, *305*, 2000475.
- (21) Chen, Y.; Yu, Z.; Ye, Y.; Zhang, Y.; Li, G.; Jiang, F. Superelastic, Hygroscopic, and Ionic Conducting Cellulose Nanofibril Monoliths by 3D Printing. *ACS Nano* **2021**, *15*, 1869–1879.
- (22) Zhang, X.; Sheng, N.; Wang, L.; Tan, Y.; Liu, C.; Xia, Y.; Nie, Z.; Sui, K. Supramolecular nanofibrillar hydrogels as highly stretchable, elastic and sensitive ionic sensors. *Mater. Horiz.* **2019**, *6*, 326–333.
- (23) Choi, D. Y.; Kim, M. H.; Oh, Y. S.; Jung, S. H.; Jung, J. H.; Sung, H. J.; Lee, H. W.; Lee, H. M. Highly Stretchable, Hysteresis-Free Ionic Liquid-Based Strain Sensor for Precise Human Motion Monitoring. *ACS Appl. Mater. Interfaces* **2017**, *9*, 1770–1780.
- (24) Fastier-Wooler, J.; Dinh, T.; Dau, V. T.; Dao, D. V. Soft ionic liquid multi-point touch sensor. *RSC Adv.* **2019**, *9*, 10733–10738.
- (25) Lin, J.; Zhu, Z.; Cheung, C. F.; Yan, F.; Li, G. Digital manufacturing of functional materials for wearable electronics. *J. Mater. Chem. C* **2020**, *8*, 10587–10603.
- (26) Li, G. Direct laser writing of graphene electrodes. *J. Appl. Phys.* **2020**, *127*, No. 010901.
- (27) Cai, G.; Hao, B.; Luo, L.; Deng, Z.; Zhang, R.; Ran, J.; Tang, X.; Cheng, D.; Bi, S.; Wang, X.; Dai, K. Highly Stretchable Sheath-Core Yarns for Multifunctional Wearable Electronics. *ACS Appl. Mater. Interfaces* **2020**, *12*, 29717–29727.
- (28) Liu, X.; Lu, C.; Wu, X.; Zhang, X. Self-healing strain sensors based on nanostructured supramolecular conductive elastomers. *J. Mater. Chem. A* **2017**, *5*, 9824–9832.
- (29) Jin, H.; Xie, M.; Wang, W.; Jiang, L.; Chang, W.; Sun, Y.; Xu, L.; Zang, S.; Huang, J.; Yan, Y.; Jiang, L. Pressing-Induced Caking: A General Strategy to Scale-Span Molecular Self-Assembly. *CCS Chemistry* **2020**, *2*, 98–106.
- (30) Wang, W.; Xie, M.; Jin, H.; Zhi, W.; Liu, K.; Ma, C.; Liao, P.; Huang, J.; Yan, Y. The pressing-induced formation of a large-area supramolecular film for oil capture. *Materials Chemistry Frontiers* **2020**, *4*, 1530–1539.
- (31) Zhu, P.; Kuang, Y.; Wei, Y.; Li, F.; Ou, H.; Jiang, F.; Chen, G. Electrostatic self-assembly enabled flexible paper-based humidity sensor with high sensitivity and superior durability. *Chem. Eng. J.* **2021**, *404*, 127105.
- (32) Zhu, P.; Liu, Y.; Fang, Z.; Kuang, Y.; Zhang, Y.; Peng, C.; Chen, G. Flexible and Highly Sensitive Humidity Sensor Based on Cellulose

Nanofibers and Carbon Nanotube Composite Film. *Langmuir* **2019**, *35*, 4834–4842.

(33) He, Y.; Ming, Y.; Li, W.; Li, Y.; Wu, M.; Song, J.; Li, X.; Liu, H. Highly Stable and Flexible Pressure Sensors with Modified Multi-Walled Carbon Nanotube/Polymer Composites for Human Monitoring. *Sensors* **2018**, *18*, 1338.

(34) Tai, Y.; Lubineau, G. Human-Finger Electronics Based on Opposing Humidity-Resistance Responses in Carbon Nanofilms. *Small* **2017**, *13*, 1603486.

(35) Tannarana, M.; Pataniya, P. M.; Bhakhar, S. A.; Solanki, G. K.; Valand, J.; Narayan, S.; Patel, K. D.; Jha, P. K.; Pathak, V. M. Humidity Sensor Based on Two-Dimensional SnSe₂/MWCNT Nanohybrids for the Online Monitoring of Human Respiration and a Touchless Positioning Interface. *ACS Sustainable Chem. Eng.* **2020**, *8*, 12595–12602.

(36) Zhao, Q.; Yuan, Z.; Duan, Z.; Jiang, Y.; Li, X.; Li, Z.; Tai, H. An ingenious strategy for improving humidity sensing properties of multi-walled carbon nanotubes via poly-L-lysine modification. *Sens. Actuators, B* **2019**, *289*, 182–185.

(37) Miao, L.; Wan, J.; Song, Y.; Guo, H.; Chen, H.; Cheng, X.; Zhang, H. Skin-Inspired Humidity and Pressure Sensor with a Wrinkle-on-Sponge Structure. *ACS Appl. Mater. Interfaces* **2019**, *11*, 39219–39227.

(38) Xie, R.; Sugime, H.; Noda, S. Dispersing and doping carbon nanotubes by poly(p-styrene-sulfonic acid) for high-performance and stable transparent conductive films. *Carbon* **2020**, *164*, 150–156.